Prospects for measurements with strange hadrons at LHCb

A.A. Alves Junior,[a] **M.O. Bettler,**[b] **A. Brea Rodríguez,**[a] **A. Casais Vidal,**[a]
V. Chobanova,[a] **X. Cid Vidal,**[a] **A. Contu,**[c] **G. D'Ambrosio,**[d] **J. Dalseno,**[a] **F. Dettori,**[e,1]
V.V. Gligorov,[f] **G. Graziani,**[g] **D. Guadagnoli,**[h] **T. Kitahara,**[i,j] **C. Lazzeroni,**[k]
M. Lucio Martínez,[a] **M. Moulson,**[l] **C. Marín Benito,**[m] **J. Martín Camalich,**[n,o]
D. Martínez Santos,[a] **J. Prisciandaro,**[a] **A. Puig Navarro,**[p] **M. Ramos Pernas,**[a]
V. Renaudin,[m] **A. Sergi**[k] and **K.A. Zarebski**[k]

[a] *Instituto Galego de Física de Altas Enerxías (IGFAE), Santiago de Compostela, Spain*

[b] *Cavendish Laboratory, University of Cambridge, Cambridge, United Kingdom*

[c] *INFN Sezione di Cagliari, Cagliari, Italy*

[d] *INFN Sezione di Napoli, Napoli, Italy*

[e] *Oliver Lodge Laboratory, University of Liverpool, Liverpool, United Kingdom*

[f] *LPNHE, Sorbonne Université, Université Paris Diderot, CNRS/IN2P3, Paris, France*

[g] *INFN Sezione di Firenze, Firenze, Italy*

[h] *Laboratoire d'Annecy-le-Vieux de Physique Théorique, Annecy Cedex, France*

[i] *Institute for Theoretical Particle Physics (TTP), Karlsruhe Institute of Technology, Kalsruhe, Germany*

[j] *Institute for Nuclear Physics (IKP), Karlsruhe Institute of Technology, Kalsruhe, Germany*

[k] *School of Physics and Astronomy, University of Birmingham, Birmingham, United Kingdom*

[l] *INFN Laboratori Nazionali di Frascati, Frascati, Italy*

[m] *Laboratoire de l'Accelerateur Lineaire (LAL), Orsay, France*

[n] *Instituto de Astrofísica de Canarias and Universidad de La Laguna, Departamento de Astrofísica, La Laguna, Tenerife, Spain*

[o] *CERN, CH-1211, Geneva 23, Switzerland*

[p] *Physik-Institut, Universität Zürich, Zürich, Switzerland*

---

[1] Now at: Università degli Studi di Cagliari, Cagliari, Italy.

E-mail: antonio.augusto.alves.junior@cern.ch,
Marc-Olivier.Bettler@cern.ch, alexandre.brea.rodriguez@cern.ch,
adrian.casais.vidal@cern.ch, veronika.chobanova@cern.ch,
xabier.cid.vidal@cern.ch, Andrea.Contu@cern.ch,
giancarlo.dambrosio@na.infn.it, jeremy.peter.dalseno@cern.ch,
francesco.dettori@cern.ch, Vladimir.Gligorov@cern.ch,
Giacomo.Graziani@cern.ch, diego.guadagnoli@cern.ch,
teppeik@kmi.nagoya-u.ac.jp, Cristina.Lazzeroni@cern.ch,
miriam.lucio.martinez@cern.ch, matthew.moulson@cern.ch,
carla.marin.benito@cern.ch, jorge.martin.camalich@cern.ch,
Diego.Martinez.Santos@cern.ch, Jessica.Prisciandaro@cern.ch,
albert.puig@cern.ch, miguel.ramos.pernas@cern.ch,
victor.daussy-renaudin@physics.ox.ac.uk, Antonino.Sergi@cern.ch,
kristian.alexander.zarebski@cern.ch

ABSTRACT: This report details the capabilities of LHCb and its upgrades towards the study of kaons and hyperons. The analyses performed so far are reviewed, elaborating on the prospects for some key decay channels, while proposing some new measurements in LHCb to expand its strangeness research program.

Contents

1 Introduction

The study of strange-hadron decays has fuelled discoveries in particle physics for the past seventy years. For instance, experimental anomalies in the strange sector motivated the prediction of the charm quark via the Glashow-Iliopoulos-Maiani (GIM) mechanism, while the discovery of CP violation prompted the postulation of the beauty and top quarks within the Cabibbo-Kobayashi-Maskawa (CKM) paradigm; all now key ingredients of the Standard Model (SM). Presently, strangeness decays are valuable probes in the search for dynamics Beyond the Standard Model (BSM), being particularly relevant in searches for sources of quark flavour violation beyond the CKM matrix. Since $s \to d$ transitions have the strongest suppression factor, they can typically probe energy scales higher than those accessible in

charm or beauty-hadron decays for couplings of comparable size [1]. Nevertheless, flavour physics experiments have greatly enhanced such knowledge from charm and beauty decays in recent years, while few measurements of strange-hadron decays have been updated or performed for the first time.

Several dedicated experiments exist for specific measurements, however few experiments possess the potential to construct a comprehensive program on the study of strange hadrons. In this work, it is argued that the LHCb experiment has the capacity, both in terms of detector performance and statistics, to produce leading measurements exploiting almost all strange-hadron species, particularly in the search for their rare decays. An overview of the current results and prospects of strangeness decays at LHCb is given, demonstrating LHCb's unique reach as a strangeness factory and motivating further research in this area. In fact, the LHCb collaboration has already published the world's most precise measurements in $K_S^0 \to \mu^+\mu^-$ [2, 3] and $\Sigma^+ \to p\mu^+\mu^-$ [4], while projecting world-leading results for $K_S^0 \to \pi^0\mu^+\mu^-$ [5] and $K_S^0 \to \pi^+\pi^-e^+e^-$ [6]. Experiments such as BESIII [7], NA62 [8, 9], KLOE2 [10], KOTO [11, 12] and CLAS [13–15] further enrich the field with diverse and complementary research programs of their own.

This document is organised as follows: section 2 is dedicated to the discussion of the production of strange-hadron decays at LHC and its detection in LHCb. Section 3 summarises the results and prospects of LHCb for several rare decays of strange hadrons. The capabilities for the measurement of the K^+ mass as well as for the study of semileptonic hyperon decays are presented in section 4, while conclusions are drawn in section 6.

2 Production and detection of strange hadrons

The LHCb detector [16] is a single-arm forward spectrometer, covering the pseudorapidity range $2 < \eta < 5$, collecting data in proton-proton collisions at the Large Hadron Collider at CERN. It is composed of a silicon-strip vertex detector surrounding the pp interaction region (VELO), with a length of about 1 metre from the interaction point, a large-area silicon-strip detector (TT) located upstream of a dipole magnet and three tracking stations of silicon-strip detectors and straw drift tubes placed downstream of the magnet. Particle identification is provided by two ring-imaging Cherenkov detectors, an electromagnetic and a hadronic calorimeter, and a muon system composed of alternating layers of iron and multiwire proportional chambers. LHCb has collected so far an integrated luminosity of about 8 fb^{-1}.

The LHCb detector will be upgraded for the next run of the LHC. This upgrade, hereafter referred to as Phase-I, includes a completely new tracking system with a pixel-based VELO [17], the Upstream Tracker (UT) replacing the TT and scintillating fibre detectors acting as tracking stations [17]. The Phase-I detector will collect on the order of 50 fb^{-1} of integrated luminosity [18]. An Expression of Interest for a second upgrade, hereafter denoted as Phase-II, can be found in ref. [19]. It is intended that on the order of 300 fb^{-1} of integrated luminosity will be collected with this upgrade.

The production of strange hadrons at LHC is exceedingly abundant. Physics projections are derived from simulated events invoking the Pythia software generator [20], where
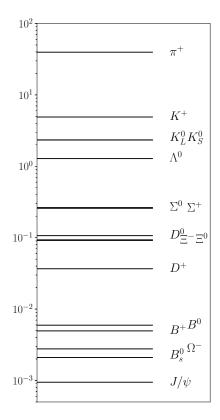
Figure 1. Multiplicity of particles produced in a single *pp* interaction at $\sqrt{s} = 13\,\text{TeV}$ within LHCb acceptance.

proton-proton collisions are configured with a centre-of-mass energy $\sqrt{s} = 13\,\text{TeV}$ and an average of one interaction per collision. The conclusions of this study are unaffected for other anticipated LHC collision energies of 14 TeV even up to 28 TeV. Multiplicities of various particles are estimated from these events in a broad LHCb geometric acceptance of pseudorapidity $\eta \in [1, 6]$, prior to any simulated detector response. This multiplicity is shown for strange hadrons in figure 1 alongside an assortment of well-known heavy flavoured hadrons for comparison. Multiple kaons and about one hyperon per event are expected to be produced in these interactions, which is roughly two and three orders of magnitude greater than for charmed and beauty hadrons, respectively. Thus, the LHCb experiment will have at its disposal the statistics necessary both for precision measurements of strange-hadron decays and for searches for their rare decays.

The efficiency of detecting strange-hadron decays will, however, not be the same as for heavy flavour for several reasons. The detector layout, which is optimised for *b* decays, implies a relatively lower acceptance for K_S^0, with K_L^0 and K^+ efficiencies diminished even further. This is due to the differing flight lengths of the different mesons. The typical decay length of a *B* meson is $\sim 1\,\text{cm}$, K_S^0 can fly a distance of nearly one metre, while $K^\pm$ and K_L^0 traverse distances longer than the full LHCb detector length on average. Flight distance distributions achieved by various strange hadrons before decaying are also obtained from Pythia simulations, which are displayed within the context of the LHCb detector in figure 2.

Depending on the decay position of a given particle, its charged decay products can be reconstructed in LHCb exploiting the relevant tracking sub-detectors. The different track categories are defined in ref. [17] as:

- long tracks: when all possible tracking information from the VELO to the T stations is available, implying that the mother particle decayed within about 1 metre of the pp interaction point;

- downstream tracks: where only the TT and T stations register tracks, allowing strange hadrons to be reconstructed with decay lengths up to about 2 metres from the interaction point.

In order to provide an estimate of the reconstruction efficiencies for long tracks, the published $K_S^0 \to \mu^+ \mu^-$ analysis from LHCb is taken as a benchmark [3]. Events with a decay time t in the range of $t/\tau_S \in [0.10, 1.45]$ were used, where τ_S is the K_S^0 lifetime. From these numbers, one could simply obtain

$$\frac{\epsilon_{K_L^0}}{\epsilon_{K_S^0}} \approx 3.5 \times 10^{-3} \quad ,$$

for the ratio of K_L^0 to K_S^0 efficiencies, $\epsilon_{K_L^0}$ and $\epsilon_{K_S^0}$, respectively.

However, as the acceptance inside the VELO is not uniform, larger lifetimes result in lower reconstruction efficiencies, further reducing $\epsilon_{K_L^0}$ next to $\epsilon_{K_S^0}$. This can be approximated by an exponential acceptance or so-called 'beta factor' $\epsilon(t) \sim e^{-\beta t}$ [21], with $\beta \sim 86\,\mathrm{ns}^{-1}$ in the case of $K_S^0 \to \mu^+ \mu^-$ decays [22]. In this case, the reduction factor becomes

$$\frac{\epsilon_{K_L^0}}{\epsilon_{K_S^0}} = \frac{\Gamma_L \displaystyle\int_{0.1\tau_S}^{1.45\tau_S} e^{-t(\Gamma_S + \beta)} dt}{\Gamma_S \displaystyle\int_{0.1\tau_S}^{1.45\tau_S} e^{-t(\Gamma_L + \beta)} dt} \approx 2.2 \times 10^{-3}, \tag{2.1}$$

where Γ_S and Γ_L are the K_S^0 and K_L^0 decay widths. Assuming that the same acceptance parametrisation used in eq. (2.1) holds also for $K^\pm$, the relative efficiency of $K^\pm$ decays with respect to K_S^0 decays is then at the level of 1%. On the other hand, the use of downstream tracks can allow for an increased lifetime acceptance. The transverse momenta of the products of strangeness decays, significantly softer than for b-hadron decays, are also detrimental to their detection at LHCb. While b-hadron decay products generally have a transverse momenta of around 1-2 GeV/c, for s-hadron decays the range is more in the region of 100-200 MeV/c. The acceptances for several benchmark channels, as well as invariant-mass resolutions, are estimated in the following applying a simplified simulation of the LHCb upgrade tracking, based on the detector descriptions found in refs. [17, 23, 24]. The following selection criteria are applied to all decay channels: the daughter particles are required to have a track impact parameter to primary vertex of greater than 400 microns, a momentum greater than 3000 MeV/c with transverse momentum greater than 80 MeV/c, while the reconstructed hadron is required to have a decay time greater than 8.9 ps and a flight distance in the plane transverse to the beam greater than 3 mm. These requirements are based on the Run 2 trigger for detached soft dimuons [25] and on the lower decay
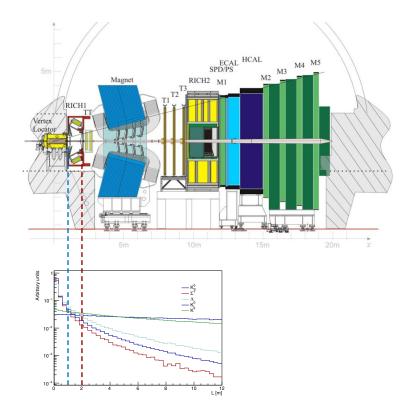
Figure 2. A side view of the LHCb detector layout [16] compared with the decay length of strange hadrons in pp collisions at $\sqrt{s} = 13\,\text{TeV}$. The blue (1m) and red (2m) dashed lines indicate the approximate distance from the interaction point at which daughter tracks can be reconstructed as long and downstream tracks, respectively.

time requirement from ref. [2]. These requirements are expected to be realistic also for future data-acquisition periods in LHCb. Acceptances are then normalised to that of fully reconstructed $K_\text{S}^0 \to \mu^+\mu^-$, which is found to be around 1%. The results of this simplified simulation are given in table 1, where the efficiency is shown using long tracks only (ϵ_L) and using downstream tracks only (ϵ_D), along with the invariant-mass resolution for each reconstruction method. The efficiency scale factors for charged hadrons with at least 300 MeV/c and electrons with over 200 MeV/c transverse momenta are also normalised to fully reconstructed $K_\text{S}^0 \to \mu^+\mu^-$ and indicated in parentheses. As neutral particles like the photon, neutrino and π^0 are not reconstructed in this study, the invariant mass of particular strange hadrons is calculated with additional kinematic constraints.

Absolute efficiencies depend significantly on the fidelity of the momentum spectra provided by Pythia, hence it is preferred to quote only relative acceptances here. As bremsstrahlung corrections are important in electron reconstruction, such modes are shown separately in table 2, in which the reference channel for efficiency normalisation is $K_\text{S}^0 \to \pi^+\pi^-e^+e^-$. The reconstruction and selection efficiency for $K_\text{S}^0 \to \pi^+\pi^-e^+e^-$ has been estimated with full LHCb simulation to be $\sim 1 \times 10^{-4}$ in ref. [6]. Lepton Flavour Violating (LFV) modes are listed in table 3, normalised to $K_S^0 \to \mu^+e^-$.

Channel	$\mathcal{R}$	ϵ_L	ϵ_D	$\sigma_L(\mathrm{MeV}/c^2)$	$\sigma_D(\mathrm{MeV}/c^2)$
$K^0_S \to \mu^+\mu^-$	1	1.0 (1.0)	1.8 (1.8)	~ 3.0	~ 8.0
$K^0_S \to \pi^+\pi^-$	1	1.1 (0.30)	1.9 (0.91)	~ 2.5	~ 7.0
$K^0_S \to \pi^0\mu^+\mu^-$	1	0.93 (0.93)	1.5 (1.5)	~ 35	~ 45
$K^0_S \to \gamma\mu^+\mu^-$	1	0.85 (0.85)	1.4 (1.4)	~ 60	~ 60
$K^0_S \to \mu^+\mu^-\mu^+\mu^-$	1	0.37 (0.37)	1.1 (1.1)	~ 1.0	~ 6.0
$K^0_L \to \mu^+\mu^-$	~ 1	2.7 (2.7) $\times 10^{-3}$	0.014 (0.014)	~ 3.0	~ 7.0
$K^+ \to \pi^+\pi^+\pi^-$	~ 2	9.0 (0.75) $\times 10^{-3}$	41 (8.6) $\times 10^{-3}$	~ 1.0	~ 4.0
$K^+ \to \pi^+\mu^+\mu^-$	~ 2	6.3 (2.3) $\times 10^{-3}$	0.030 (0.014)	~ 1.5	~ 4.5
$\Sigma^+ \to p\mu^+\mu^-$	~ 0.13	0.28 (0.28)	0.64 (0.64)	~ 1.0	~ 3.0
$\Lambda \to p\pi^-$	~ 0.45	0.41 (0.075)	1.3 (0.39)	~ 1.5	~ 5.0
$\Lambda \to p\mu^-\bar{\nu}_\mu$	~ 0.45	0.32 (0.31)	0.88 (0.86)	$-$	$-$
$\Xi^- \to \Lambda\mu^-\bar{\nu}_\mu$	~ 0.04	39 (5.7) $\times 10^{-3}$	0.27 (0.09)	$-$	$-$
$\Xi^- \to \Sigma^0\mu^-\bar{\nu}_\mu$	~ 0.03	24 (4.9) $\times 10^{-3}$	0.21 (0.068)	$-$	$-$
$\Xi^- \to p\pi^-\pi^-$	~ 0.03	0.41(0.05)	0.94 (0.20)	~ 3.0	~ 9.0
$\Xi^0 \to p\pi^-$	~ 0.03	1.0 (0.48)	2.0 (1.3)	~ 5.0	~ 10
$\Omega^- \to \Lambda\pi^-$	~ 0.001	95 (6.7) $\times 10^{-3}$	0.32 (0.10)	~ 7.0	~ 20

Table 1. Acceptance scale factors ϵ, and mass resolutions σ, for only long (L) and only downstream (D) tracks obtained from our simplified description of the LHCb Upgrade tracking system geometry. The production ratio of the strange hadron with respect to K^0_S is shown as $\mathcal{R}$. All efficiencies are normalised to that of fully reconstructed $K^0_S \to \mu^+\mu^-$ and averaged over particles and anti-particles. Channels containing a photon, neutrino and π^0 are partially reconstructed.

Channel	$\mathcal{R}$	ϵ_L	ϵ_D	$\sigma_L(\mathrm{MeV}/c^2)$	$\sigma_D(\mathrm{MeV}/c^2)$
$K^0_S \to \pi^+\pi^-e^+e^-$	1	1.0 (0.18)	2.83 (1.1)	~ 2.0	~ 10
$K^0_S \to \mu^+\mu^-e^+e^-$	1	1.18 (0.48)	2.93 (1.4)	~ 2.0	~ 11
$K^+ \to \pi^+e^+e^-$	~ 2	0.04 (0.01)	0.17 (0.06)	~ 3.0	~ 13
$\Sigma^+ \to pe^+e^-$	~ 0.13	1.76 (0.56)	3.2 (1.3)	~ 3.5	~ 11
$\Lambda \to p\pi^-e^+e^-$	~ 0.45	$< 2.2 \times 10^{-4}$	~ 17 (< 2.2) $\times 10^{-4}$	$-$	$-$

Table 2. Acceptance scale factors ϵ, and mass resolutions σ, for only long (L) and only downstream (D) tracks obtained from our simplified description of the LHCb Upgrade tracking system geometry. All efficiencies are normalised to that of fully reconstructed $K^0_S \to \pi^+\pi^-e^+e^-$ and are averaged between particles and anti-particles. The invariant-mass resolutions shown in the table correspond to the ideal case of perfect bremsstrahlung recovery.

Channel	$\mathcal{R}$	ϵ_L	ϵ_D	$\sigma_L(\mathrm{MeV}/c^2)$	$\sigma_D(\mathrm{MeV}/c^2)$
$K^0_S \to \mu^+e^-$	1	1.0 (0.84)	1.5 (1.3)	~ 3.0	~ 8.0
$K^0_L \to \mu^+e^-$	1	3.1 (2.6) $\times 10^{-3}$	13 (11) $\times 10^{-3}$	~ 3.0	~ 7.0
$K^+ \to \pi^+\mu^+e^-$	~ 2	3.1 (1.1) $\times 10^{-3}$	16 (8.5)$\times 10^{-3}$	~ 2.0	~ 8.0

Table 3. Acceptance scale factors ϵ, and mass resolutions σ, for only long (L) and only downstream (D) tracks obtained from our simplified description of the LHCb Upgrade tracking system geometry. All efficiencies are normalised to that of fully reconstructed $K^0_S \to \mu^+e^-$ and averaged between particles and anti-particles. The invariant-mass resolutions shown in the table correspond to the ideal case of perfect bremsstrahlung recovery.

2.1 Trigger

The current trigger of LHCb has three stages, a hardware stage (L0) and two software stages (HLT1 and HLT2). The L0 is practically unchangeable and implies an efficiency loss of roughly 80% of reconstructible strange-hadron decays involving muons [25]. For non muonic final states it implies a loss of about 90% to 99%, due to the much larger transverse energy trigger thresholds for hadrons and electrons [26], depending on whether also events triggered by the underlying event (and not by the considered signal) are accepted or not [27]. During Run 1, the total trigger efficiency for strangeness decays was 1–2% or lower, depending on the final state. The main reason for those low efficiencies is the soft transverse momentum spectrum of strange-hadron decay products. During Run 2, dedicated software triggers for strange-hadron decays into dimuons have been implemented with an overall improvement of about one order of magnitude in the total trigger efficiency achieved with respect to Run 1 [25]. In the Upgrade of the LHCb experiment, the trigger is expected to be entirely software based with L0 removed, hence $\mathcal{O}(1)$ efficiencies are attainable.[1] It has been shown in simulation that for dimuon final states, the output rate can be kept under control for transverse momentum thresholds as low as 80 MeV/c without any significant signal loss [5]. Although the dimuon final state is the cleanest signature from an experimental perspective, trigger algorithms for other final states are possible and are currently under investigation. As an example, a software trigger for dielectrons from strange decays was already implemented during Run 2 [6] and will serve as a basis for the Upgrade.

2.2 Flavour tagging

As pointed out in ref. [28], $K_{\rm S}^0$-$K_{\rm L}^0$ interference has an effective lifetime which is only twice that of the $K_{\rm S}^0$ and thus has an enhanced acceptance in LHCb compared to pure $K_{\rm L}^0$ decays. By tagging the initial flavour of the K^0, access to $K_{\rm L}^0$ physics and CP phenomena in the $K_{\rm S}^0 - K_{\rm L}^0$ system is permitted through these interference effects.[2] Though not used for this paper, it is valuable to mention the possibility of strange-hadron flavour tagging at LHCb through K^0 processes such as $pp \to K^0 K^- X$, $pp \to K^{*+} X \to K^0 \pi^+ X$ and $pp \to K^0 \Lambda^0 X$.

3 Rare decays

Rare decays are excellent probes for BSM. On the theoretical side, the SM background to each process is small by definition, while experimentally, measurements are typically statistically limited, but this limitation can constantly be improved. In this section, the status and prospects for several benchmark rare decays of different strange-hadron species are shown.

---

[1]Here and in the following, trigger efficiencies are calculated and referred to events that have passed the full offline selection, hence perfect efficiencies are attainable when the trigger requirements are aligned to, or looser than, the offline selection.

[2]While the present paper is focused mainly on rare and semileptonic decays, a program of measurements of CP violation in the $K_{\rm S}^0 - K_{\rm L}^0$ system is in principle possible and merits further study.

3.1 Rare decays of K_S^0 mesons

Due to its shorter lifetime compared to K_L^0 and K^+, the K_S^0 meson is the most accessible in terms of reconstruction in LHCb. With a geometric acceptance at the 1% level and a production cross section of about 0.3 barn, the LHCb Phase-II upgrade could reach branching fraction sensitivities down to the level of 10^{-15} in the ideal case of perfect selection and trigger with no background. In the following, the channels LHCb has already investigated are discussed in addition to new analysis suggestions.

3.1.1 $K_S^0 \to \mu^+\mu^-$

In the SM, the $K_S^0 \to \mu^+\mu^-$ decay is dominated by long-distance (LD) effects with subdominant short-distance (SD) contributions coming from Z-penguin and W-box diagrams. Yet in absolute terms, the long-distance contribution is still minute with the decay rate highly suppressed [28–30]. The theoretical prediction,

$$\mathcal{B}(K_S^0 \to \mu^+\mu^-)_{\text{SM}} = (5.18 \pm 1.50_{\text{LD}} \pm 0.02_{\text{SD}}) \times 10^{-12} \quad ,$$

when compared with the current experimental upper limit [3]

$$\mathcal{B}(K_S^0 \to \mu^+\mu^-) < 8 \times 10^{-10} \text{ at } 90\% \text{ CL} \quad ,$$

leaves room for small BSM contributions to interfere and compete with the SM rate. This is shown to be the case in leptoquark (LQ) models [31, 32] as well as in the Minimal Supersymmetric Standard Model (MSSM) [33]. In the LQ case, the enhancements can reach as high as the current experimental bound, while within the MSSM, $\mathcal{B}(K_S^0 \to \mu^+\mu^-)$ can adopt values anywhere in the range $[0.78, 35.00] \times 10^{-12}$, even surpassing the experimental bound in certain narrow, finely-tuned regions of the parameter space [33]. This can be seen in figure 3, where $A_{L\gamma\gamma}^{\mu}$ indicates the long-distance contribution to $\mathcal{B}(K_L^0 \to \mu^+\mu^-)$. The CP asymmetry of this decay is also sensitive to BSM contributions, but experimentally accessible only by means of a tagged analysis.

The LHCb prospects for the search for $K_S^0 \to \mu^+\mu^-$ decays are excellent. With only 2011 data, the experiment improved the previous world upper limit by a factor of thirty [2] and recently gained another factor of ten [3]. In the case of an LHCb Phase-II upgrade running during the proposed HL-LHC era, the full software trigger will allow an exploration of branching fractions below the 10^{-11} regime. Figure 4, first shown in ref. [34], shows the expected upper limit of $\mathcal{B}(K_S^0 \to \mu^+\mu^-)$ as a function of the integrated luminosity scaled by the trigger efficiency, based on the extrapolation given in ref. [3]. This demonstrates that if the trigger efficiency is near ~ 1, as can be achieved technically with the Phase-I full software trigger, LHCb could exclude branching fractions down towards the vicinity of the SM prediction.

3.1.2 $K_S^0 \to \pi^0\mu^+\mu^-$

The experimental uncertainty on $\mathcal{B}(K_S^0 \to \pi^0\mu^+\mu^-)$ is the dominant uncertainty on the SM prediction of $\mathcal{B}(K_L^0 \to \pi^0\mu^+\mu^-)$, the latter being an important channel for BSM searches,
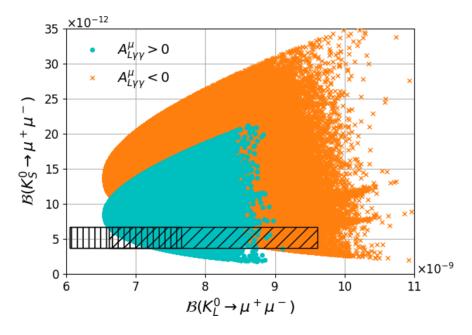
Figure 3. A generic scan of $\mathcal{B}(K_S^0 \to \mu^+\mu^-)$ vs. $\mathcal{B}(K_L^0 \to \mu^+\mu^-)$ from ref. [33], in an MSSM scenario with universal gaugino masses. The cyan dots correspond to predictions with $A_{L\gamma\gamma}^\mu > 0$ and the orange crosses to predictions using $A_{L\gamma\gamma}^\mu < 0$. The vertically hatched area corresponds to the SM prediction for $A_{L\gamma\gamma}^\mu > 0$ while the diagonally hatched area corresponds to the SM prediction for $A_{L\gamma\gamma}^\mu < 0$.
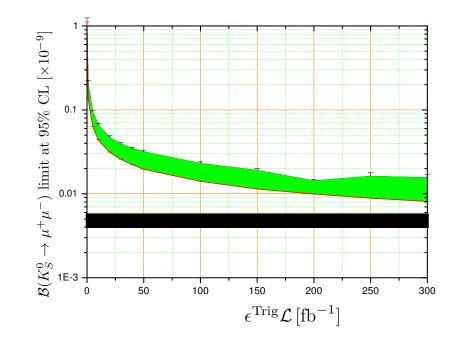

Figure 4. Expected upper limit of $\mathcal{B}(K_S^0 \to \mu^+\mu^-)$ from LHCb including upgrades, against the product of the integrated luminosity and trigger efficiency, taken from ref. [34]. The LHCb upgrade is expected to collect 50fb^{-1}, and the Phase-II $\approx 300\text{fb}^{-1}$.

such as extra dimensions [35]. Currently, the only existing measurement comes from the NA48 experiment [36],

$$\mathcal{B}(K_{\mathrm{S}}^0 \to \pi^0 \mu^+ \mu^-) = (2.9^{+1.5}_{-1.2} \pm 0.2) \times 10^{-9} \quad .$$

The upgraded LHCb experiment can quickly eclipse NA48 in terms of precision on $\mathcal{B}(K_{\mathrm{S}}^0 \to \pi^0 \mu^+ \mu^-)$ and achieve a level of 0.25×10^{-9} with 50 fb^{-1} of integrated luminosity and assuming 100% trigger efficiency [5] (see footnote 1).

Aside from the branching fraction, the differential decay rate in the dimuon mass possesses interesting information. As the electromagnetic structure of this decay in the SM receives only a single contribution from the vector current, an amplitude analysis cannot offer any advantages over a fit to the dimuon mass spectrum alone. The decay dynamics of this channel are assumed to be governed by a linear dependence in q^2, thus there are two free, real parameters of the model, which can be determined from data, a_S and b_S, where b_S is the coefficient of the linear term in q^2. This complements the information available from the branching fraction, which has the form,

$$\mathcal{B}(K_{\mathrm{S}}^0 \to \pi^0 \mu^+ \mu^-) \propto 0.07 - 4.52 a_S - 1.5 b_S + 98.7 a_S^2 + 57.7 a_S b_S + 8.95 b_S^2 \quad ,$$

in the SM [37].

Importantly, a_S is the relevant parameter for the SM determination of $\mathcal{B}(K_{\mathrm{L}}^0 \to \pi^0 \mu^+ \mu^-)$. It has been estimated from the NA48 measurement of $\mathcal{B}(K_{\mathrm{S}}^0 \to \pi^0 \mu^+ \mu^-)$ that $|a_S| = 1.2 \pm 0.2$ [35], assuming vector meson dominance (VMD), where $b_S/a_S = m_K^2/m_\rho^2$. Without VMD, resolving a_S with only a single observable is not possible. Hence, as the precision in $\mathcal{B}(K_{\mathrm{S}}^0 \to \pi^0 \mu^+ \mu^-)$ increases, use of the q^2 dependence, which has been calculated in ref. [37], becomes a viable approach in avoiding this model dependence.

Two degenerate solutions are expected for both a_S and b_S. A pseudo-experiment study indicates that the significance of the sign-flip in a_S is consistent with zero even up to signal yields well beyond the reach of any proposed LHC upgrade. Although the model-dependent expectation is that the product $a_S b_S$, is preferred to be positive, the proximity to zero of the b_S solution corresponding to negative a_S renders this constraint untenable.

A number of analysis configurations from a purely statistical point of view are considered, neglecting systematic uncertainties. The statistical power has been obtained from the expected sensitivity in $\mathcal{B}(K_{\mathrm{S}}^0 \to \pi^0 \mu^+ \mu^-)$, where the signal plus background yield is translated into an effective signal-only yield. Firstly, the scenario where both a_S and b_S are measured from the q^2 distribution is considered. An additional constraint coming from NA48 is also considered, which relates the branching fraction of $K_{\mathrm{S}}^0 \to \pi^0 e^+ e^-$, to a_S and b_S through

$$\mathcal{B}(K_{\mathrm{S}}^0 \to \pi^0 e^+ e^-) = [0.01 - 0.76 a_S - 0.21 b_S + 46.5 a_S^2 + 12.9 a_S b_S + 1.44 b_S^2] \times 10^{-10} \quad .$$

The uncertainty on a_S using the value of b_S motivated by VMD is also investigated. In this paradigm, it becomes possible to measure a_S from the $K_{\mathrm{S}}^0 \to \pi^0 \mu^+ \mu^-$ yield alone, which is tested as the final case.

Configuration	Phase I	Phase II
BR & q^2 fit	0.25	0.10
BR & q^2 fit with NA48 constraint	0.19	0.10
BR & q^2 fit fixing b_S	0.06	0.024
a_S measurement from BR alone	0.06	0.024

Table 4. Projected statistical uncertainties on a_S under various analysis conditions.

The reach of LHCb in each of these scenarios is summarised in table 4 for different effective yields. In the case that b_S is measured from the data, its uncertainties are expected to be 0.87 (0.35) for the Phase-I (Phase-II) data samples. The results show that with the effective events from Phase-I data, the constraint coming from NA48 on the $K_S^0 \to \pi^0 e^+ e^-$ branching fraction will play a role in reducing the uncertainty on a_S, while with Phase-II data, the uncertainty will be entirely dominated by the LHCb $K_S^0 \to \pi^0 \mu^+ \mu^-$ measurement. The results also indicate the vast improvement in a_S that becomes possible at the expense of model independence and demonstrate that the q^2 distribution has very little impact on the overall uncertainty on a_S when b_S is fixed. Further improvements could, of course, come from an LHCb measurement of $K_S^0 \to \pi^0 e^+ e^-$.

3.1.3 $K_S^0 \to \pi^+ \pi^- e^+ e^-$ and other K_S^0 dielectron modes

With a relatively high branching fraction of $\sim 5 \times 10^{-5}$ [38], the $K_S^0 \to \pi^+ \pi^- e^+ e^-$ decay offers an excellent opportunity to study rare decays of K_S^0 mesons to electrons at LHCb. Due to bremsstrahlung, electrons are generally more difficult to reconstruct than other particles, such as pions or muons. This is especially the case for low momentum electrons, such as those expected in K_S^0 decays. Given the branching fraction of $K_S^0 \to \pi^+ \pi^- e^+ e^-$, a significant yield per fb^{-1} is expected to be produced within the LHCb acceptance, thus this decay could be used both for CP-violation studies [38] and to search for potential resonant structure in the $e^+ e^-$ invariant-mass spectrum. From a purely experimental standpoint, it is interesting for the study of both the reconstruction and identification of low momentum electrons and to harness as a normalisation channel for various 4-body K_S^0 rare decays. Examples include decays to four leptons, which could be sensitive to the presence of BSM contributions [39], suppressed SM decays such as $K_S^0 \to \pi^+ \pi^- \mu^+ \mu^-$, or Lepton Flavour Violating decays like $K_S^0 \to \mu^+ \mu^+ e^- e^-$ and $K_S^0 \to \pi^+ \pi^- \mu^+ e^-$. Moreover, $K_S^0 \to \pi^+ \pi^- e^+ e^-$ could present as a prominent background in these searches, ergo, a comprehensive understanding of its expected yield and invariant-mass distribution becomes crucial.

The $K_S^0 \to \pi^+ \pi^- e^+ e^-$ decay at LHCb is studied in ref. [6]. This analysis involves a generic study of the decay using LHCb simulated samples and includes a search with the Run 1 data, giving prospects for Run 2 and Run 3. The LHCb hardware trigger is found to limit observation of this decay, with only $\sim$100 candidates per fb^{-1} expected to be reconstructed and selected in Run 1 and Run 2. Despite this relatively low yield, it is also concluded that a purpose-built offline selection, including the use of a Multi-Variate Analysis (MVA) classifier, could lead to an observation of the signal. The prospects for Run 3 are much better, with an expected yield at the level of $\sim 50 \times 10^3$ selected candidates
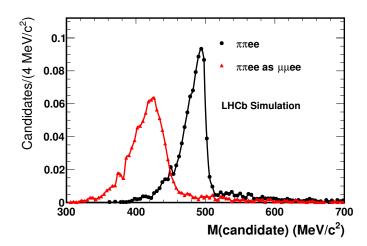
Figure 5. Expected invariant-mass shape of $K_S^0 \to \pi^+\pi^- e^+e^-$ shown additionally with the $\mu^+\mu^- e^+e^-$ mass hypothesis, taken from ref. [6].

per fb^{-1}. Furthermore, the presence of $K_S^0 \to \pi^+\pi^- e^+e^-$ as a background for 4-lepton final states is also studied. Figure 5, taken from ref. [6], shows the invariant-mass shape of the $K_S^0 \to \pi^+\pi^- e^+e^-$ decay in conjunction with the alternate $\mu^+\mu^- e^+e^-$ mass hypothesis, to highlight its separation with respect to a potential $K_S^0 \to \mu^+\mu^- e^+e^-$ signal, both obtained from simulation. While both peaks are separated, a significant contamination from $K_S^0 \to \pi^+\pi^- e^+e^-$ is expected in the signal region due to the long tails of the distribution and the much larger yield expected for this mode. However this contribution can be modelled from simulation and systematic effects controlled with data, in analogy to the contamination of $K_S^0 \to \pi^+\pi^-$ decays as a background for $K_S^0 \to \mu^+\mu^-$ [3].

The presence of electron bremsstrahlung combined with the low transverse momentum of the final state particles, makes the invariant-mass resolution of this final state significantly worse when compared to $K_S^0 \to \mu^+\mu^-$, for instance. New reconstruction strategies could enhance the sensitivity of LHCb to $K_S^0 \to \pi^+\pi^- e^+e^-$ and other similar final states, such as those mentioned above. Given that the position of the K_S^0 production and decay vertices can be determined, the invariant-mass resolution of the K_S^0 could be calculated ignoring the absolute momentum of one of the four final state particles through relativistic kinematic constraints. This is advantageous as the invariant-mass resolution becomes less dependent on bremsstrahlung, given that the direction of electrons in the VELO is barely influenced by such effects. In addition, this technique could allow a more efficient reconstruction of these electrons, using tracks not required to have a segment after the magnet. Taking into account that the VELO pattern recognition efficiency is at the level of $\sim 70\%$ [40], even for tracks with $p \sim \mathcal{O}(1\,\text{MeV}/c)$, improvements in the reconstruction efficiency up to a factor of 10 could be theoretically possible.

3.1.4 $K_S^0 \to \gamma\mu^+\mu^-$, $K_S^0 \to X^0\mu^+\mu^-$ and $K_S^0 \to X^0\pi^\pm\mu^\mp$

The analysis strategy of $K_S^0 \to \pi^0\mu^+\mu^-$ can be applied to any $K_S^0 \to X^0\mu^+\mu^-$ mode, where X^0 is an arbitrary neutral system. The performance of the search will be strongly related
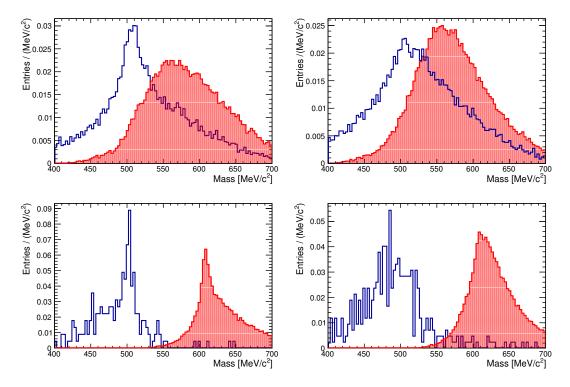
Figure 6. Reconstructed invariant mass for $K_S^0 \to \gamma\mu^+\mu^-$ (top) and $K_S^0 \to \pi^0\mu^+\mu^-$ (bottom) obtained from simulation. The $K_S^0 \to \gamma\mu^+\mu^-$ and $K_S^0 \to \pi^0\mu^+\mu^-$ signal events are shown with a solid blue line and the $K_S^0 \to \pi^+\pi^-$ background is illustrated with red filled histograms. The left side portrays events reconstructed with long tracks, while reconstruction with downstream tracks are depicted on the right.

to the mass of the neutral system, with heavier X^0 leading to superior invariant-mass resolution of the K_S^0 peak. The resolution is studied here using simulated $K_S^0 \to \gamma\mu^+\mu^-$ decays, corresponding to the most restrictive case of a massless X^0. This decay is predicted in the SM to occur with a branching fraction of $(1.45 \pm 0.27) \times 10^{-9}$ [41]. Background from generated $K_S^0 \to \pi^+\pi^-$ is also considered with the aforementioned simplified tracking emulation. From figure 6, the distinction between signal and background is visibly worse for $K_S^0 \to \gamma\mu^+\mu^-$ than it is for $K_S^0 \to \pi^0\mu^+\mu^-$. Nevertheless, both peaks show clear separation and hence the search is feasible. A reduction of the $K_S^0 \to \pi^+\pi^-$ background is possible by requiring the dimuon candidate to point away from the primary vertex, in the same way as is done in $K_S^0 \to \pi^0\mu^+\mu^-$ analysis [5]. A similar strategy can be embraced in $K_S^0 \to X^0\pi^\pm\mu^\mp$, where the X^0 in this case could be some neutrino, either from the SM decay $K_S^0 \to \pi^\pm\mu^\mp\nu$ or a heavy BSM neutrino (see also section 4.2.1).

3.2 Rare decays of K^+ mesons

From the efficiency ratios of table 1 and considering that sensitivities for K_S^0 branching fractions are at the 10^{-10}-10^{-12} level, sensitivities from 10^{-7}-10^{-10} could be expected for K^+ decays, depending on the background level. For K^+ mesons, which are electrically charged and long-lived, the possibility to interact with one or more VELO stations can lead to an

additional source of discrimination against combinatorial background [42]. Single event sensitivities could then well reach below 10^{-12}, in the case of very small background (muonic channels), while taking into account higher levels of background, possible sensitivities of order 10^{-10}–10^{-11} are foreseen.

3.2.1 $K^+ \to \pi^+\mu^+\mu^-$ and $K^+ \to \pi^+e^+e^-$

The decays $K^\pm \to \pi^\pm\mu^+\mu^-$ are flavour-changing processes induced at the one-loop level, which are well suited to explore SM structure and its extensions. These decays are dominated by long-distance contributions involving one photon exchange *i.e.* $K \to \pi\gamma^* \to \pi\mu^+\mu^-$. The branching fraction has been derived within the framework of Chiral Perturbation Theory (χ_{PT}) in terms of a vector-interaction form factor, which describes the single-photon exchange and characterises the dimuon invariant-mass spectrum [37, 43, 44]. The differential decay rate can be written as a kinematic term depending on masses and 4-momenta, multiplied by $|W(z)|^2$, where W is the form factor and $z = (m_{\mu\mu}/M_K)^2$. The form factor is given by $W(z) \propto W_{\text{pol}}(z)W_{\pi\pi}(z)$, where the second term represents the tiny contribution from the two-pion-loop intermediate state and the first term is phenomenologically described by a polynomial. As the form factor is required to vanish at lowest order in the low-energy chiral expansion, the polynomial term takes the form $W_{\text{pol}}(z) = (a_+ + b_+z)$, where a_+ and b_+ are free parameters of the model to be determined by experiment. In a similar fashion to $b \to s$ transitions, $s \to d$ processes can be described with an effective Lagrangian depending on Wilson coefficients, generating only the non-zero Wilson coefficients C_{7A} and C_{7V} for the semileptonic operators. Such coefficients can be split into SM and BSM contributions. In particular, a_+ can be written as a function of the Wilson coefficient C_{7A} [45], leading to potential constraints on BSM. A further comparison of the electron and muon channels would provide an additional test of Lepton Flavour Universality and further constrain BSM dynamics.

Natural extensions of the SM involve the inclusion of sterile neutrinos which mix with ordinary neutrinos. An example is the Neutrino Minimal Standard Model (νMSM) [46], which can be further extended by adding a scalar field to incorporate inflation and provide a common source for electroweak symmetry breaking and right-handed neutrino masses [47]. The new particles predicted by these models can be produced in charged kaon decays. Notably, the two-unit Lepton Number Violating (LNV) $K^\pm \to \pi^\mp\mu^\pm\mu^\pm$ decay could proceed via an off-shell or on-shell Majorana neutrino [48], while an inflaton could be produced in the Lepton Number Conserving (LNC) $K^\pm \to \pi^\pm X$, decaying promptly to $X \to \mu^+\mu^-$ [49].

The NA48/2 collaboration [50, 51] reports the most precise measurement to date of the branching fraction and provide limits on the Majorana neutrino and inflaton. They measured

$$\mathcal{B}(K^\pm \to \pi^\pm\mu^+\mu^-) = (9.62 \pm 0.21_{\text{stat}} \pm 0.13_{\text{syst}}) \times 10^{-8},$$
$$\mathcal{B}(K^\pm \to \pi^\mp\mu^\pm\mu^\pm) < 8.6 \times 10^{-11} \ (90\% \ \text{CL}),$$
$$\mathcal{B}(K^\pm \to \pi^\pm X) < 10^{-11}\text{-}10^{-9} \ (90\% \ \text{CL}),$$

where the range depends on the assumed resonance lifetime. The NA62 experiment plans to improve on all these measurements and limits, though with positively-charged kaons only [8].
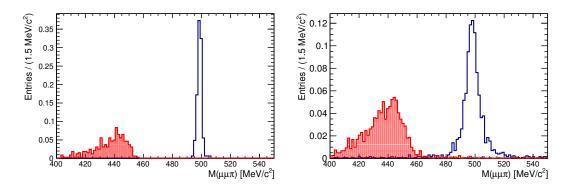
Figure 7. Reconstructed invariant mass for $K^+ \to \pi^+\mu^+\mu^-$, where signal events are shown with a solid blue line and $K^+ \to \pi^+\pi^+\pi^-$ background illustrated by red filled histograms. The left side gives events reconstructed with long tracks, while reconstruction with downstream tracks are pictured on the right.

The LHCb mass resolution is sufficient to separate these decays from the kinematically similar $K^+ \to \pi^+\pi^+\pi^-$, as illustrated in figure 7. LHCb can acquire large $K^+ \to \pi^+\mu^+\mu^-$ signal yields as table 1 and figure 1 clearly indicate. Assuming $\mathcal{O}(1)$ trigger efficiencies, a yield of $\mathcal{O}(10^4)$ fully reconstructed and selected signal events is expected per year of upgraded-LHCb data taking, even considering only long-track candidates. This suggests $K^+ \to \pi^+\mu^+\mu^-$ decays would provide an early opportunity for a measurement to demonstrate the potential of the upgraded detector for these channels. Similar arguments apply to the $K^+ \to \pi^+e^+e^-$ mode, whose somewhat lower reconstruction efficiency due to the presence of electrons is negated by its larger branching fraction. Rigorous control over the systematic uncertainties will be paramount in order to improve the current world-average precision of 3% on the electron mode. If successful, the full spectrum of both channels will afford a highly precise test of Lepton Flavour Universality.

3.3 Tests of LFV

Modes with LFV, such as $K \to (n\pi)\mu^\pm e^\mp$ form null tests of the SM. Sizeable BSM contributions to such decays have garnered increased attention in recent times because of hints at Lepton Universality Violation (LUV) in $B \to K^{(*)}\ell^\pm\ell^\mp$ processes. In fact, both classes of processes can be generated by new contributions to the product of two neutral currents, involving down-type quarks and leptons respectively, the only difference being the strength of the flavour couplings involved.

From the amount of LUV alluded to in $B \to K^{(*)}\ell^\pm\ell^\mp$, one may expect $B \to K^{(*)}$ LFV rates of the order of 10^{-8} using general effective-theory (EFT) arguments [52]. More quantitative estimates require the introduction of a flavour model [45, 53–64]. As discussed in ref. [65], such arguments can be extended to the $K \to (\pi)\mu^\pm e^\mp$ case, with fairly general assumptions on the different flavour couplings involved. Expected rates can be as large as 10^{-10} - 10^{-13} for the $K_L \to \mu^\pm e^\mp$ mode and a factor of ~ 100 smaller for $K^+ \to \pi^+\mu^\pm e^\mp$. Taking into account the suppression mechanisms at play, such 'large' rates are a non-trivial finding. Their relatively wide range is due to the inherent model dependence especially in

the choice of the leptonic coupling and the overall scale of the new interaction, typically between 5 and 15 TeV [65]. Since limits on the branching fractions for the $K \to \pi e\mu$ modes were pushed down to the level of $10^{-11} - 10^{-12}$ in the 1990s, there has been no significant further progress on the experimental side, with the current limits at 90% CL,

$$\begin{aligned}
\mathcal{B}(K_L \to e^\pm \mu^\mp) &< 4.7 \times 10^{-12} \quad [66], &\quad \mathcal{B}(K_L \to \pi^0 e^\pm \mu^\mp) &< 7.6 \times 10^{-11} \quad [67], \\
\mathcal{B}(K^+ \to \pi^+ e^- \mu^+) &< 1.3 \times 10^{-11} \quad [68], &\quad \mathcal{B}(K^+ \to \pi^+ e^+ \mu^-) &< 5.2 \times 10^{-10} \quad [69],
\end{aligned} \tag{3.1}$$

being decades old.

These modes can be profitably pursued at the upgraded LHCb, benefiting from huge strange-production yields. In fact, starting from a total $K^\pm$ cross section of 0.63 barns and taking into account the fraction of kaons in the pseudorapidity acceptance of LHCb, one can estimate a $K^\pm$ cross section as large as 0.14 barns. Ref. [65] presents a feasibility study of the modes listed in eq. (3.1), taking $K^+ \to \pi^+ \mu^\pm e^\mp$ as a benchmark. It can be seen that LHCb may be able to update the existing limits and probe a sizeable part of the parameter space suggested by the discrepancies in B physics.

3.4 Rare decays of Σ hyperons

LHCb has recently published the most precise search for $\Sigma^+ \to p\mu^+\mu^-$ [4], showing strong evidence for this decay with 4.1σ significance. A measurement of the branching fraction is reported along with a dimuon invariant-mass distribution consistent with SM predictions, challenging the so-called HyperCP-anomaly [70]. This measurement was based on Run 1 data, where no trigger path existed specifically for this channel. As discussed in ref. [25], Run 2 will have a dedicated trigger both at the HLT1 and HLT2 levels, where about an order of magnitude increase in the trigger efficiency is anticipated. With a signal yield in excess of 150 events, Run 2 data will allow a measurement of the differential decay rate and possibly other observables with recent predictions such as the forward-backward asymmetry [71]. Applying similar reasoning on the trigger efficiency as with other decays in this document, on the order of a thousand signal decays could be measured per year of data taking with an upgraded LHCb detector, opening the possibility for precision measurements of direct CP violation. Assuming similar reconstruction and selection efficiencies, a search for the lepton and baryon number violating $\Sigma^+ \to \bar{p}\mu^+\mu^+$ decay could also be performed, reaching an expected branching fraction sensitivity on the order of 10^{-9}.

While of great interest, it will be difficult for LHCb to improve the precision on the branching fraction of the radiative $\Sigma^+ \to p\gamma$ decay, whose world average is currently $\mathcal{B}(\Sigma^+ \to p\gamma) = (1.23 \pm 0.05) \times 10^{-3}$ [72]. On the other hand, the ability to reconstruct the $\Sigma^+ \to p\pi^0$ decay, which has similar topology in the detector, has already been demonstrated [4]. This implies that the $\Sigma^+ \to p\gamma$ decay could be useful as an alternative normalisation channel, particularly in a possible search for $\Sigma^+ \to pe^+e^-$ decays. By virtue of the electron mass, this channel receives a larger contribution from long-distance photon contributions compared to $\Sigma^+ \to p\mu^+\mu^-$, for a predicted branching fraction of $\mathcal{B}(\Sigma^+ \to pe^+e^-) \in [9.1, 10.1] \times 10^{-6}$ [73]. The only experimental information available on this channel dates back to 1969 where three events where observed leading to an upper limit of 7×10^{-6} at 90% CL [74]. Unsurprisingly,
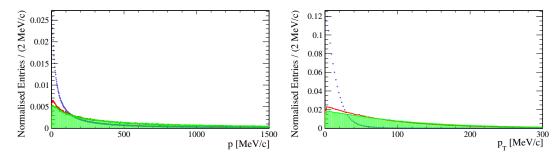
Figure 8. Momentum (left) and transverse momentum (right) for electrons generated in various strangeness decays, where the dotted blue represents $\Lambda \to p\pi^- e^+ e^-$, solid red $K_s^0 \to \pi^+\pi^- e^+ e^-$ and filled green $K_s^0 \to \mu^+\mu^- e^+ e^-$.

this yield is not yet distinguishable from converted-photon $\Sigma^+ \to p\gamma$ decays. Although electron reconstruction is more difficult, it is expected that the LHCb experiment could improve on this measurement and perhaps reach the SM level already with Run 2 data. Analogously, the LFV decays $\Sigma^+ \to p e^\pm \mu^\mp$ could also be searched for with similar sensitivity.

Owing to the extreme difficulty of reconstructing neutrons, the LHCb experiment will most likely not contribute towards the study of the Σ^- hyperon, barring exotic channels with baryon number violation.

As far as Σ^0 particles are concerned, these do not have a sizeable decay time, due to their electromagnetic decay into $\Lambda\gamma$, therefore they would decay at the production vertex in LHCb. For this reason while our simplified model could predict their reconstruction efficiency, the sensitivity for Σ^0 decays would be dominated by primary interaction background, which would require a full simulation to be understood. We therefore do not provide estimates on these sensitivities. We limit ourselves to suggest that LHCb could attempt a first search for the $\Sigma^0 \to \Lambda e^+ e^-$ decay, for which no experimental measurement is currently available, despite the fact that several authors proposed this decay to study parity violation in strangeness-conserving weak currents [75–77]. In lieu of an experimental measurement the PDG reports a theoretical calculation driven by internal photon conversions for an expected branching fraction of about 5×10^{-3} [78], easily reachable by LHCb if background can be controlled.

3.5 Rare decays of Λ hyperons

The most compelling contribution LHCb could offer in the realm of Λ hyperon is the improvement on the branching fraction of the radiative $\Lambda \to p\pi^-\gamma$ decay, whose measured value $\mathcal{B}(\Lambda \to p\pi^-\gamma) = (8.4 \pm 1.4) \times 10^{-4}$, is known only for pion centre-of-mass momenta less than 95 MeV/c [79]. In addition, first studies of $\Lambda \to p\pi^- e^+ e^-$, which proceeds via flavour-changing neutral currents could be possible, reaching branching fractions of $10^{-6} - 10^{-7}$. A major challenge for $\Lambda \to p\pi^- e^+ e^-$ is the extremely low transverse electron momentum as illustrated in figure 8, translating into a meagre reconstruction efficiency in accordance with table 2. The corresponding channel with muons in this case would be phase-space forbidden.

LHCb can also advance the study of baryon-number-violating decays, which can be produced by virtual particles with masses at the Grand Unified Theory (GUT) scale. For weakly decaying particles, this would imply branching fractions suppressed proportionally to $(m_W/\Lambda_{\mathrm{GUT}})^4$, in principle placing observation out of reach for LHCb and any other experiment. These decays are also indirectly constrained by severe limits from nucleon decays. The CLAS collaboration has recently reported searches for several baryon-number-violating Λ decays [80]. Most of these are in the form $\Lambda \to h\ell$, where h is a K^+ or π^+ meson and $\ell = e, \mu$ leptons. CLAS then provided the first direct experimental limits on such branching fractions to be in the range $[10^{-7}, 10^{-6}]$. LHCb can certainly improve on most of these limits, reaching sensitivities around the 10^{-9} level already with Run 2 data.

3.6 Rare decays of hyperons with multiple strangeness

In addition to hadrons with one strange quark or anti-quark ($|S| = 1$), LHCb will also produce a large number of baryons with more strange quarks, namely the Ξ and Ω hyperons. As can be seen from figure 1, the production of Ξ is in the region of charmed mesons, while Ω production is further suppressed, due to the additional strange quark, to the level around the beauty meson. Nevertheless, this provides a large dataset with which to improve existing measurements on these hadrons.

In the context of rare decays, the main interest for $|S| > 1$ hyperons is for $\Delta S = 2$ transitions, which are practically forbidden in the SM, with branching fractions of order 10^{-17}. Potential NP transitions mediated by parity-odd low-energy operators may enhance the observed rates while respecting constraints from $K^0 - \bar{K}^0$ mixing [81]. In this respect, the LHCb experiment has the capabilities to improve the branching fraction of $\Xi^0 \to p\pi^-$, which has an upper limit of 8.2×10^{-6} at 90% CL obtained at the HyperCP experiment [82]. This decay has an experimental signature completely reminiscent of the corresponding Λ decay, which is selected even without particle identification at LHCb [83], making it the ideal calibration sample for $\Xi^0 \to p\pi^-$. Therefore, there is no doubt that the background to this channel could be rejected with high signal retention. Branching fractions of order $10^{-9} - 10^{-10}$ could be reached with LHCb Upgrade data.

In similar vein, the $\Omega \to \Lambda\pi^-$ decay has an upper limit on the branching fraction of 2.9×10^{-6} at 90% CL also placed by the HyperCP experiment [82]. The sensitivity to this channel is again expected to be improved over the current limit given its clean topology, down to branching fractions of order $10^{-8} - 10^{-9}$. Incidentally, the channel $\Xi^- \to p\pi^-\pi^-$, which has an upper limit of only 3.7×10^{-4} at 90% CL [84], will also be easily improved by LHCb, similarly to $\Xi^0 \to p\pi^-$, reaching sensitivities of order 10^{-9}.

4 Other measurements with strange-hadron decays

4.1 Measurement of the K^+ meson mass

Due to its superb tracking performance, the LHCb detector is particularly suited for a precision measurement of the charged kaon mass. The current experimental average of the K^+ meson mass is $m_{K^+} = 493.677 \pm 0.013$ MeV/c^2 [72]. The uncertainty is dominated

by the disagreement between the two most precise measurements, both performed using kaonic atom transitions [85, 86]. Despite the relatively low acceptance in LHCb, the large production cross section for strange mesons in pp collision allows for a large number of $K^+ \to \pi^+\pi^-\pi^+$ candidates to be fully reconstructed with an excellent signal-to-background ratio [42]. The number of fully reconstructed decays occurring within the VELO acceptance is estimated to be of $\mathcal{O}(10^7)/\text{fb}^{-1}$ for pp collisions at $\sqrt{s} = 13\,\text{TeV}$ with a relatively good mass resolution of $\lesssim 4$ MeV/c^2 [4]. Therefore, the statistical error on the mass is expected to be below 10^{-3} MeV/c^2 with the entire LHCb dataset. The main systematic uncertainty, which is expected to limit the final precision, will most likely come from the knowledge of the momentum scale resolution, which is proportional to the Q-value of the decay, $m_{K^+} - 3m_{\pi^\pm} \approx 75\,\text{MeV}/c^2$. For $K^+ \to \pi^+\pi^-\pi^+$, this systematic should be below 0.02 MeV/c^2 [87], making this measurement competitive with the world average.

4.2 Semileptonic decays

The latest results from semileptonic $b \to c$ transitions suggest the possibility of BSM contributions in charged-current quark decays breaking Lepton Flavour Universality (LFU) [88]. Hence, it is natural to investigate if similar patterns can be found in $s \to u$ transitions.

4.2.1 Semileptonic $K_{\rm S}^0$ decays

A search for the $K_{\rm S}^0 \to \pi^\pm\mu^\mp\nu$ process, which is as yet unobserved experimentally, could be performed at LHCb. This would be useful as a measurement of LFU when comparing to the well-known $K_{\rm S}^0 \to \pi^\pm e^\mp\nu$ decay [72]. Depending on the precision achieved, the measurement of this branching fraction could also be useful in constraining the CKM matrix element $|V_{us}|$ [89]. However, LHCb would need excellent control over the systematics to reach the $< 1\%$ level of precision that would be required for such a measurement to be competitive. The most challenging background for this search is expected to arise from the corresponding $K_{\rm L}^0$ decay to the same final state. The much larger branching fraction of the $K_{\rm L}^0$ decay, $\sim 27\%$ [72], compensates the reduction in efficiency due to the longer $K_{\rm L}^0$ lifetime, leading to significant yields still deposited within the LHCb acceptance: considering the expected $K_{\rm S}^0 \to \pi^\pm\mu^\mp\nu$ branching fraction, $(4.69 \pm 0.05) \times 10^{-4}$ [72], the ratio of $K_{\rm L}^0$ to $K_{\rm S}^0$ events in this final state in the LHCb acceptance is expected to be about 1.5 (4.5) when using long (downstream) tracks, without further selection. However, given the precise knowledge of the $K_{\rm L}^0$ branching fraction, $(27.04 \pm 0.07)\%$ [72], this contribution could be statistically subtracted leaving only a small systematic uncertainty.

4.2.2 Semileptonic hyperon decays

Semileptonic hyperon decays have been shown to be sensitive to BSM scalar and tensor contributions [90]. The branching fractions of such hyperon decays, which are copiously produced at the LHC, show uncertainties at the $20\% - 100\%$ level leaving vast room for progress. For example, $\mathcal{B}(\Lambda \to p\mu^-\bar{\nu_\mu}) = (1.57 \pm 0.35) \times 10^{-4}$, $\mathcal{B}(\Xi^- \to \Lambda\mu^-\bar{\nu_\mu}) = 3.5^{+3.5}_{-2.2} \times 10^{-4}$ and $\mathcal{B}(\Xi^- \to \Sigma^0\mu^-\bar{\nu_\mu}) < 8 \times 10^{-4}$ at 90% CL.

Those decays would be partially reconstructed in LHCb, as was shown in section 2, with improved measurements directly translating into tighter bounds on LFU, since the electron
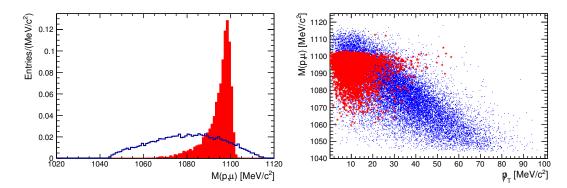
Figure 9. The left plot shows the reconstructed invariant mass for $\Lambda \to p\mu^-\bar{\nu}_\mu$ candidates. Signal events are given by a solid blue line, while the $\Lambda \to p\pi^-$ background is displayed in filled red. The right figure shows a scatter plot of the reconstructed mass vs. missing momentum in the plane transverse to the Λ flight direction for signal (blue squares) and $\Lambda \to p\pi^-$ background (red stars). Final state radiation in the Λ decay vertex is not included in the simulation.

modes have already been measured very precisely. Kinematic constraints such as those applied in the $K_S^0 \to \pi^0\mu^+\mu^-$ analysis can be used to reconstruct the strange-baryon peak. Since the expected yields for strange semileptonic decays are large, the main challenge is not the trigger efficiency, but is instead the discrimination against peaking backgrounds like $\Lambda \to p\pi^-$ or $\Xi^- \to \Lambda\pi^-$. The mass of the p, μ candidates from $\Lambda \to p\mu^-\bar{\nu}_\mu$ and misidentified $\Lambda \to p\pi^-$ is shown in figure 9, which also plots the dependency of the mass against the estimated missing momentum transverse to the Λ flight direction. Clearly, the signal and peaking background provide contrasting signatures. It has to be noted, however, that neither final state radiation in the Λ decay nor the decay in flight of the pion are included in the simulation, both of which are effects that can partially dilute the discriminating power of the missing transverse momentum. A similar study is performed for $\Xi^- \to \Lambda\mu^-\bar{\nu}_\mu$, which also demonstrates the separation between signal and the corresponding peaking-background distribution from $\Xi^- \to \Lambda\pi^-$ decays, as depicted in figure 10.

5 Competition from other experiments

Competition from other experiments on strange-hadron decays will be scarce in the coming years. We briefly review it in the following. The NA48 experiment has contributed significantly to the physics of strange-hadron decays, but has already analysed their full dataset on rare K_S^0 and hyperon decays (e.g. refs [36, 38, 91, 92]) and we are not aware of any plan to exploit it further. The NA62 experiment will give fundamental results on charged kaons, however it will not have a neutral beam at its disposal before 2026. In particular, NA62 may reach the 10^{-12} ballpark in LFV kaon decays [93] with the data collected so far. The KLOE2 experiment will most probably be able to contribute on semileptonic measurements, in addition to its core CP-violation program, and possibly measure the K^+ mass, but will not have enough statistics for rare decays. The CLAS experiment could possibly contribute again to searches on rare hyperon decays, but will not be competitive with LHCb below the 10^{-7} level in branching fraction. Similarly it is not expected to
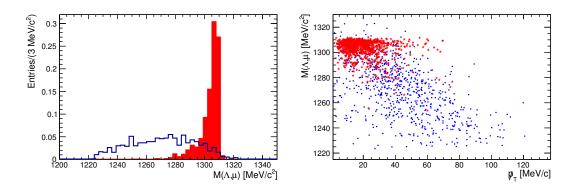
Figure 10. The left plot shows the reconstructed invariant mass for $\Xi^- \to \Lambda \mu^- \bar{\nu}_\mu$ candidates. Signal events are given by a solid blue line, while the $\Xi^- \to \Lambda \pi^-$ background is displayed in filled red. The right figure shows a scatter plot of the reconstructed mass vs. missing momentum in the plane transverse to the Ξ^- flight direction for signal (blue squares) and $\Lambda \to p\pi^-$ background (red stars). Final state radiation in the Ξ^- and Λ decay vertices is not included in the simulation.

contribute on K_S^0 decays. Finally, flavour factories such as BESIII and BelleII can possibly contribute to the physics of rare strange-hadron decays. The BESIII collaboration has for example published a search for $\eta' \to K\pi$ decays [94], reaching a branching fraction limit of order 10^{-4}. We are not aware of any published physics result from the Belle collaboration on rare strange hadron decays and this topic is not mentioned in BelleII physics book [95]. In addition, there are new proposed facilities such as TauFV [96] which may be able to reach $\mathcal{O}(10^{19})$ kaons in the decay volume, with a detector layout comparable to that of LHCb, for which however we are not aware of more in-depth sensitivity studies on the decay modes discussed in this paper. However, we would welcome an increase in the interest for strange physics and would consider competition from these collaborations to be a very healthy development indeed.

6 Conclusions

The decays of strange particles become increasingly important as the energy scale for dynamics beyond the Standard Model increases. The LHCb experiment has provided the world's best measurements in $K_S^0 \to \mu^+\mu^-$ and $\Sigma^+ \to p\mu^+\mu^-$ decays with excellent prospects for expanding its research program on strangeness decays. For the first time, this paper reports estimates of detection efficiencies for several K_S^0, $K^\pm$ and hyperon decay channels and evaluates the invariant-mass resolution that could be achieved with the full and downstream tracking systems, while demonstrating the capacity of LHCb to resolve signal from potential peaking-background distributions. The results show that several promising new measurements are feasible in various K_S^0, $K^\pm$ and hyperon decays with diverse final states.

Acknowledgments

References

[1] Y. Nir, *Probing new physics with flavor physics (and probing flavor physics with new physics)*, in the proceedings of the *Prospects in Theoretical Physics (PiTP) summer program on The Standard Model and Beyond*, June 16–27, IAS, Princeton, U.S.A. (2007), arXiv:0708.1872 [INSPIRE].

[2] LHCb collaboration, *Search for the rare decay $K_S^0 \to \mu^+ \mu^-$*, *JHEP* **01** (2013) 090 [CERN-PH-EP-2012-267].

[3] LHCb collaboration, *Improved limit on the branching fraction of the rare decay $K_S^0 \to \mu^+ \mu^-$*, *Eur. Phys. J.* **C 77** (2017) 678 [LHCb-PAPER-2017-009].

[4] LHCb collaboration, *Evidence for the rare decay $\Sigma^+ \to p \mu^+ \mu^-$*, *Phys. Rev. Lett.* **120** (2018) 221803 [LHCb-PAPER-2017-049].

[5] V.G. Chobanova et al., *Sensitivity of LHCb and its upgrade in the measurement of $\mathcal{B}(K_S^0 \to \pi^0 \mu^+ \mu^-)$*, LHCb-PUB-2016-017 (2016).

[6] C. Marin Benito, L. Garrido Beltran, and X. Cid Vidal, *Feasibility study of $K_S^0 \to \pi^+ \pi^- e^+ e^-$ at LHCb* , LHCb-PUB-2016-016 (2016).

[7] H.-B. Li, *Prospects for rare and forbidden hyperon decays at BESIII*, *Front. Phys. (Beijing)* **12** (2017) 121301 [arXiv:1612.01775] [INSPIRE].

[8] NA62 collaboration, *2018 NA62 status report to the CERN SPSC*, CERN-SPSC-2018-010 (2018).

[9] NA62 collaboration, *The beam and detector of the NA62 experiment at CERN*, 2017 *JINST* **12** P05025 [arXiv:1703.08501] [INSPIRE].

[10] G. Amelino-Camelia et al., *Physics with the KLOE-2 experiment at the upgraded DAϕNE*, *Eur. Phys. J.* **C 68** (2010) 619 [arXiv:1003.3868] [INSPIRE].

[11] J. Comfort et al., *Proposal for $K_L^0 \to \pi^0 \bar\nu \bar\nu$ experiment at J-Parc*, http://j-parc.jp/researcher/Hadron/en/pac_0606/pdf/p14-Yamanaka.pdf.

[12] KOTO collaboration, *Search for the $K_L \to \pi^0 \nu \bar\nu$ and $K_L \to \pi^0 X^0$ decays at the J-Parc KOTO experiment*, *Phys. Rev. Lett.* **122** (2019) 021802 [arXiv:1810.09655] [INSPIRE].

[13] CLAS collaboration, https://www.jlab.org/Hall-B/clas-web/.

[14] CLAS12 collaboration, https://www.jlab.org/Hall-B/clas12-web/.

[15] CLAS collaboration, *The CEBAF Large Acceptance Spectrometer (CLAS)*, *Nucl. Instrum. Meth.* **A 503** (2003) 513 [INSPIRE].

[16] LHCb collaboration, *The LHCb detector at the LHC*, 2008 *JINST* **3** S08005 [INSPIRE].

[17] LHCb collaboration, *LHCb tracker upgrade technical design report*, CERN-LHCC-2014-001 (2014).

[18] LHCb collaboration, *Implications of LHCb measurements and future prospects*, *Eur. Phys. J.* **C 73** (2013) 2373 [arXiv:1208.3355] [INSPIRE].

[19] LHCb collaboration, *Expression of interest for a Phase-II LHCb upgrade: opportunities in flavour physics and beyond, in the HL-LHC era*, CERN-LHCC-2017-003 (2017).

[20] T. Sjöstrand, S. Mrenna and P.Z. Skands, *A brief introduction to PYTHIA 8.1*, *Comput. Phys. Commun.* **178** (2008) 852 [arXiv:0710.3820] [INSPIRE].

[21] LHCb collaboration, *Measurement of CP violation and the B_s^0 meson decay width difference with $B_s^0 \to J/\psi K^+ K^-$ and $B_s^0 \to J/\psi \pi^+ \pi^-$ decays*, *Phys. Rev.* **D 87** (2013) 112010 [CERN-PH-EP-2013-055].

[22] X. Cid Vidal, *Search for the rare decays $B_{(s)}^0 \to \mu^+\mu^-$ and $K_S^0 \to \mu^+\mu^-$ with 1 fb^{-1} at LHCb*, Ph.D. thesis, Santiago de Compostela University, Santiago de Compostela, Spain (2012).

[23] LHCb collaboration, *LHCb VELO upgrade technical design report*, CERN-LHCC-2013-021 (2013).

[24] L.B.A. Hommels, P.F. van der Heijden, M. Merk and N. Tuning, *The tracker in the trigger of LHCb*, CERN-THESIS-2006-058 (2006).

[25] F. Dettori, D. Martinez Santos, and J. Prisciandaro, *Low-p_T dimuon triggers at LHCb in Run 2*, LHCb-PUB-2017-023 (2017).

[26] A. Puig, *The LHCb trigger in 2011 and 2012*, LHCb-PUB-2014-046 (T2014).

[27] S. Tolk, J. Albrecht, F. Dettori and A. Pellegrino, *Data driven trigger efficiency determination at LHCb*, LHCb-PUB-2014-039 (2014).

[28] G. D'Ambrosio and T. Kitahara, *Direct CP violation in $K \to \mu^+\mu^-$*, *Phys. Rev. Lett.* **119** (2017) 201802 [arXiv:1707.06999] [INSPIRE].

[29] G. Ecker and A. Pich, *The longitudinal muon polarization in $K_L \to \mu^+\mu^-$*, *Nucl. Phys.* **B 366** (1991) 189 [INSPIRE].

[30] G. Isidori and R. Unterdorfer, *On the short distance constraints from $K_{L,S} \to \mu^+\mu^-$*, *JHEP* **01** (2004) 009 [hep-ph/0311084] [INSPIRE].

[31] I. Dorsner et al., *Limits on scalar leptoquark interactions and consequences for GUTs*, *JHEP* **11** (2011) 002 [arXiv:1107.5393] [INSPIRE].

[32] C. Bobeth and A.J. Buras, *Leptoquarks meet ε'/ε and rare Kaon processes*, *JHEP* **02** (2018) 101 [arXiv:1712.01295] [INSPIRE].

[33] V. Chobanova et al., *Probing SUSY effects in $K_S^0 \to \mu^+\mu^-$*, *JHEP* **05** (2018) 024 [arXiv:1711.11030] [INSPIRE].

[34] D.M. Santos, *A strange program for LHCb*, *EPJ Web Conf.* **179** (2018) 01013 [INSPIRE].

[35] M. Bauer, S. Casagrande, U. Haisch and M. Neubert, *Flavor physics in the Randall-Sundrum model: II. Tree-level weak-interaction processes*, *JHEP* **09** (2010) 017 [arXiv:0912.1625] [INSPIRE].

[36] NA48/1 collaboration, *Observation of the rare decay $K_S \to \pi^0 \mu^+ \mu^-$*, *Phys. Lett.* **B 599** (2004) 197 [`hep-ex/0409011`] [INSPIRE].

[37] G. D'Ambrosio, G. Ecker, G. Isidori and J. Portoles, *The decays $K \to \pi \ell^+ \ell^-$ beyond leading order in the chiral expansion*, *JHEP* **08** (1998) 004 [`hep-ph/9808289`] [INSPIRE].

[38] NA48/1 collaboration, *Precision measurement of the ratio $BR(K_S \to \pi^+ \pi^- e^+ e^-)/BR(K_L \pi^+ \pi^- \pi_D^0)$*, *Phys. Lett.* **B 694** (2011) 301 [INSPIRE].

[39] G. D'Ambrosio, D. Greynat and G. Vulvert, *Standard model and new physics contributions to K_L and K_S into four leptons*, *Eur. Phys. J.* **C 73** (2013) 2678 [`arXiv:1309.5736`] [INSPIRE].

[40] D. Hutchcroft, *VELO pattern recognition*, CERN-LHCb-2007-013 (2007).

[41] G. Colangelo, R. Stucki and L.C. Tunstall, *Dispersive treatment of $K_S \to \gamma\gamma$ and $K_S \to \gamma \ell^+ \ell^-$*, *Eur. Phys. J.* **C 76** (2016) 604 [`arXiv:1609.03574`] [INSPIRE].

[42] A. Contu, *A method to study long lived charged particles at LHCb*, LHCb-PUB-2014-032 (2014).

[43] S. Friot and D. Greynat, *Long-distance contributions in $K \to \pi l^+ l^-$ decays*, in the proceedings of the 40th *Rencontres de Moriond on Electroweak Interactions and Unified Theories*, March 5–12, La Thuile, Italy (2005), `hep-ph/0506018` [INSPIRE].

[44] A.Z. Dubnickova et al., *Kaon decay probe of the weak static interaction*, *Phys. Part. Nucl. Lett.* **5** (2008) 76 [`hep-ph/0611175`] [INSPIRE].

[45] A. Crivellin, G. D'Ambrosio, M. Hoferichter and L.C. Tunstall, *Violation of lepton flavor and lepton flavor universality in rare kaon decays*, *Phys. Rev.* **D 93** (2016) 074038 [`arXiv:1601.00970`] [INSPIRE].

[46] T. Asaka and M. Shaposhnikov, *The νMSM, dark matter and baryon asymmetry of the universe*, *Phys. Lett.* **B 620** (2005) 17 [`hep-ph/0505013`] [INSPIRE].

[47] M. Shaposhnikov and I. Tkachev, *The νMSM, inflation and dark matter*, *Phys. Lett.* **B 639** (2006) 414 [`hep-ph/0604236`] [INSPIRE].

[48] L.S. Littenberg and R. Shrock, *Implications of improved upper bounds on $|\Delta L| = 2$ processes*, *Phys. Lett.* **B 491** (2000) 285 [`hep-ph/0005285`] [INSPIRE].

[49] F. Bezrukov and D. Gorbunov, *Light inflaton Hunter's Guide*, *JHEP* **05** (2010) 010 [`arXiv:0912.0390`] [INSPIRE].

[50] NA48/2 collaboration, *Searches for lepton number violation and resonances in $K^\pm \to \pi \mu\mu$ decays*, *Phys. Lett.* **B 769** (2017) 67 [`arXiv:1612.04723`] [INSPIRE].

[51] NA48/2 collaboration, *New measurement of the $K^\pm \to \pi^\pm \mu^+ \mu^-$ decay*, *Phys. Lett.* **B 697** (2011) 107 [`arXiv:1011.4817`] [INSPIRE].

[52] S.L. Glashow, D. Guadagnoli and K. Lane, *Lepton flavor violation in B decays?*, *Phys. Rev. Lett.* **114** (2015) 091801 [`arXiv:1411.0565`] [INSPIRE].

[53] D. Guadagnoli and K. Lane, *Charged-lepton mixing and lepton flavor violation*, *Phys. Lett.* **B 751** (2015) 54 [`arXiv:1507.01412`] [INSPIRE].

[54] S.M. Boucenna, J.W.F. Valle and A. Vicente, *Are the B decay anomalies related to neutrino oscillations?*, *Phys. Lett.* **B 750** (2015) 367 [`arXiv:1503.07099`] [INSPIRE].

[55] A. Celis, J. Fuentes-Martin, M. Jung and H. Serodio, *Family nonuniversal Z' models with protected flavor-changing interactions*, *Phys. Rev.* **D 92** (2015) 015007 [`arXiv:1505.03079`] [INSPIRE].

[56] R. Alonso, B. Grinstein and J. Martin Camalich, *Lepton universality violation and lepton flavor conservation in B-meson decays*, *JHEP* **10** (2015) 184 [arXiv:1505.05164] [INSPIRE].

[57] B. Gripaios, M. Nardecchia and S.A. Renner, *Linear flavour violation and anomalies in B physics*, *JHEP* **06** (2016) 083 [arXiv:1509.05020] [INSPIRE].

[58] D. Bečirević, O. Sumensari and R. Zukanovich Funchal, *Lepton flavor violation in exclusive $b \to s$ decays*, *Eur. Phys. J.* **C 76** (2016) 134 [arXiv:1602.00881] [INSPIRE].

[59] D. Bečirević, N. Košnik, O. Sumensari and R. Zukanovich Funchal, *Palatable leptoquark scenarios for lepton flavor violation in exclusive $b \to s\ell_1\ell_2$ modes*, *JHEP* **11** (2016) 035 [arXiv:1608.07583] [INSPIRE].

[60] G. Hiller, D. Loose and K. Schönwald, *Leptoquark flavor patterns & B decay anomalies*, *JHEP* **12** (2016) 027 [arXiv:1609.08895] [INSPIRE].

[61] D. Bečirević and O. Sumensari, *A leptoquark model to accommodate $R_K^{\mathrm{exp}} < R_K^{\mathrm{SM}}$ and $R_{K^*}^{\mathrm{exp}} < R_{K^*}^{\mathrm{SM}}$*, *JHEP* **08** (2017) 104 [arXiv:1704.05835] [INSPIRE].

[62] D. Buttazzo, A. Greljo, G. Isidori and D. Marzocca, *B-physics anomalies: a guide to combined explanations*, *JHEP* **11** (2017) 044 [arXiv:1706.07808] [INSPIRE].

[63] S.F. King, *Flavourful Z' models for $R_{K^{(*)}}$*, *JHEP* **08** (2017) 019 [arXiv:1706.06100] [INSPIRE].

[64] M. Bordone, C. Cornella, J. Fuentes-Martín and G. Isidori, *Low-energy signatures of the* PS^3 *model: from B-physics anomalies to LFV*, *JHEP* **10** (2018) 148 [arXiv:1805.09328] [INSPIRE].

[65] M. Borsato et al., *Effective-field-theory arguments for pursuing lepton-flavor-violating K decays at LHCb*, *Phys. Rev.* **D 99** (2019) 055017 [arXiv:1808.02006] [INSPIRE].

[66] BNL collaboration, *New limit on muon and electron lepton number violation from $K_L^0 \to \mu^{\pm} e^{\mp}$ decay*, *Phys. Rev. Lett.* **81** (1998) 5734 [hep-ex/9811038] [INSPIRE].

[67] KTeV collaboration, *Search for lepton flavor violating decays of the neutral kaon*, *Phys. Rev. Lett.* **100** (2008) 131803 [arXiv:0711.3472] [INSPIRE].

[68] A. Sher et al., *An Improved upper limit on the decay $K^+ \to \pi^+ \mu^+ e^-$*, *Phys. Rev.* **D 72** (2005) 012005 [hep-ex/0502020] [INSPIRE].

[69] R. Appel et al., *Search for lepton flavor violation in K+ decays*, *Phys. Rev. Lett.* **85** (2000) 2877 [hep-ex/0006003] [INSPIRE].

[70] HyperCP collaboration, *Evidence for the decay $\Sigma^+ \to p\mu^+\mu^-$*, *Phys. Rev. Lett.* **94** (2005) 021801 [hep-ex/0501014] [INSPIRE].

[71] X.-G. He, J. Tandean and G. Valencia, *Decay rate and asymmetries of $\Sigma^+ \to p\mu^+\mu^-$*, *JHEP* **10** (2018) 040 [arXiv:1806.08350] [INSPIRE].

[72] Particle Data Group collaboration, *Review of particle physics*, *Chin. Phys.* **C 40** (2016) 100001.

[73] X.-G. He, J. Tandean and G. Valencia, *The decay $\Sigma^+ \to p\ell^+\ell^-$ within the standard model*, *Phys. Rev.* **D 72** (2005) 074003 [hep-ph/0506067] [INSPIRE].

[74] G. Ang et al., *Radiative sigma-plus-minus decays and search for neutral currents*, *Z. Phys.* **228** (1969) 151 [INSPIRE].

[75] H.S. Mani and H.S. Sharatchandra, *Effect of neutral weak current in the decay $\Sigma(0)$ to $\Lambda(0)$ e^+e^- in Weinberg's model*, *Phys. Rev.* **D 10** (1974) 2849 [INSPIRE].

[76] E.S. Abers and M. Sharif, *Parity violation in the decay* $\Sigma(0) \to \Lambda e^+ e^-$, *Phys. Rev.* **D 16** (1977) 2237 [INSPIRE].

[77] J.C. D'Olivo and M.A. Perez, *Parity violating asymmetries in the decay* $\Sigma^0 \to \Lambda e^+ e^-$, *Phys. Rev.* **D 23** (1981) 1994 [INSPIRE].

[78] G. Feinberg, *Internal pair creation in* Σ^0 *decay*, *Phys. Rev.* **109** (1958) 1019 [INSPIRE].

[79] M. Baggett et al., *A measurement of radiative* Λ *decays*, *Phys. Lett.* **B 42** (1972) 379.

[80] M.E. McCracken et al., *Search for baryon-number and lepton-number violating decays of* Λ *hyperons using the CLAS detector at Jefferson Laboratory*, *Phys. Rev.* **D 92** (2015) 072002 [arXiv:1507.03859] [INSPIRE].

[81] X.-G. He and G. Valencia, $\Delta I = 3/2$ *and* $\Delta S = 2$ *hyperon decays in chiral perturbation theory*, *Phys. Lett.* **B 409** (1997) 469 [*Erratum ibid.* **B 418** (1998) 443] [hep-ph/9705462] [INSPIRE].

[82] HYPERCP collaboration, *Search for* $\Delta S = 2$ *nonleptonic hyperon decays*, *Phys. Rev. Lett.* **94** (2005) 101804 [hep-ex/0503036] [INSPIRE].

[83] R. Aaij et al., *Selection and processing of calibration samples to measure the particle identification performance of the LHCb experiment in Run 2*, *EPJ Tech. Instrum.* **6** (2019) 1 [arXiv:1803.00824] [INSPIRE].

[84] N. Yeh et al., *Observation of rare decay modes of the* Ξ *hyperons*, *Phys. Rev.* **D 10** (1974) 3545 [INSPIRE].

[85] A.S. Denisov et al., *New measurements of the mass of the* K^- *meson*, *JETP Lett.* **54** (1991) 558 [INSPIRE].

[86] K.P. Gall et al., *Precision Measurements of the* K^- *and* Σ^- *masses*, *Phys. Rev. Lett.* **60** (1988) 186 [INSPIRE].

[87] M. Needham, *Momentum scale calibration using resonances*, CERN-LHCb-2008-037 (2008).

[88] G. Ciezarek et al., *A challenge to lepton universality in B meson decays*, *Nature* **546** (2017) 227 [arXiv:1703.01766] [INSPIRE].

[89] M. Moulson, *Experimental determination of* V_{us} *from kaon decays*, PoS(CKM2016)033 [arXiv:1704.04104] [INSPIRE].

[90] H.-M. Chang, M. González-Alonso and J. Martin Camalich, *Nonstandard semileptonic hyperon decays*, *Phys. Rev. Lett.* **114** (2015) 161802 [arXiv:1412.8484] [INSPIRE].

[91] NA48/1 collaboration, *Measurement of the branching ratio of the decay* $\Xi^0 \to \Sigma^+ \mu^- \bar{\nu}_\mu$, *Phys. Lett.* **B 720** (2013) 105 [arXiv:1212.3131] [INSPIRE].

[92] NA48 collaboration, *First observation and branching fraction and decay parameter measurements of the weak radiative decay* $\Xi^0 \to \Lambda e^+ e^-$, *Phys. Lett.* **B 650** (2007) 1 [hep-ex/0703023] [INSPIRE].

[93] NA62 collaboration, *Prospects for exotics and LFV at NA62*, *J. Phys. Conf. Ser.* **800** (2017) 012039 [INSPIRE].

[94] BESIII collaboration, *Search for the weak decay* $\eta' \to K^\pm \pi^\mp$ *and precise measurement of the branching fraction* $\mathcal{B}(J/\psi \to \phi\eta')$, *Phys. Rev.* **D 93** (2016) 072008 [arXiv:1602.07405] [INSPIRE].

[95] BELLE-II collaboration, *The Belle II physics book*, arXiv:1808.10567 [INSPIRE].

[96] G. Wilkinson et al., *TauFV*, talk given at the *Physics Beyond Colliders Working Group meeting*, June 13–14, CERN, Geneve, Switzerland (2018).